

THIRTEENTH EUROPEAN ROTORCRAFT FORUM

6.10  
Paper No. 10

THE MEASUREMENT AND CONTROL OF HELICOPTER BLADE MODAL RESPONSE  
USING BLADE-MOUNTED ACCELEROMETERS

Norman D. Ham  
Massachusetts Institute of Technology, U.S.A.  
and  
Dwight L. Balough and Peter D. Talbot  
Ames Research Center, NASA, U.S.A.

September 8-11, 1987  
ARLES, FRANCE

ASSOCIATION AERONAUTIQUE ET ASTRONAUTIQUE DE FRANCE

Norman D. Ham

Massachusetts Institute of Technology, U.S.A.

Dwight L. Balough and Peter D. Talbot

Ames Research Center, NASA, U.S.A.

ABSTRACT

The measurement of helicopter blade flapping, bending, and lag modal acceleration and displacement response using blade-mounted accelerometers is described. It is shown that knowledge of the blade mode shapes is sufficient to permit separation of the modal contributions to the accelerometer signals using matrix inversion. The application of the McKillip filter to the identification of modal rate response is described. Finally, the design of flapping, bending, and lag mode controllers utilizing the conventional swash plate is presented.

The measurement technique is illustrated using flight test results obtained using a Black Hawk helicopter.

1. INTRODUCTION

The concept of Individual-Blade-Control (IBC) embodies the control of broadband electrohydraulic actuators attached to each blade, using signals from sensors mounted on the blades to supply appropriate control commands to the actuators. Note that IBC involves not only control of each blade independently, but also a feedback loop for each blade in the rotating frame. In this manner it becomes possible to reduce the severe effects of atmospheric turbulence, retreating blade stall, blade-vortex interaction, blade-fuselage interference, and blade and rotor instabilities, while providing improved performance and flying qualities [1-10].

It is evident that the IBC system will be most effective if it is comprised of several sub-systems, each controlling a specific mode, e.g., the blade flapping mode, the first blade flatwise bending mode, and the first blade lag mode [2]. Each sub-system operates in its appropriate frequency band.

Consider the modal equation of motion

$$m\ddot{x} + c\dot{x} + kx = F(t) + AF \tag{1}$$

where the modal control force AF is

$$AF = -K_A m\ddot{x} - K_R c\dot{x} - K_P kx \tag{2}$$

on substituting (2) into (1)

$$(1+K_A)m\ddot{x} + (1+K_R)c\dot{x} + (1+K_P)kx = F(t)$$

For the case  $K_A = K_R = K_P = K$

$$m\ddot{x} + c\dot{x} + kx = [1/(1+K)] F(t)$$

and the modal response is attenuated by the factor  $1/(1+K)$  while the modal damping and natural frequency are unchanged.

For modal damping augmentation, only the rate feedback  $AF = -K_R c\dot{x}$  is required.

The configuration considered in [1-7] employs an individual actuator and multiple feedback loops to control each blade. These actuators and feedback loops rotate with the blades and, therefore, a conventional swash plate is not required. However, some applications of individual-blade-control can be achieved by placing the actuators in the non-rotating system and controlling the blades through a conventional swash plate as described in Section 6 and in [8].

This research was sponsored by the Ames Research Center, NASA, under Cooperative Agreements NCC-2-366 and NCC-2-447.

The following sections describe the design of a system controlling blade flapping, bending, and lag dynamics, and related testing of the system on a model rotor in the wind tunnel. The control inputs considered are blade pitch changes proportional to blade flapping and bending acceleration, velocity, and displacement, and lag velocity. It is then shown that helicopter gust alleviation/attitude stabilization, vibration alleviation, and IP lag damping augmentation can be achieved using the conventional helicopter swash plate for an N-bladed rotor where  $N \geq 3$ . For  $N \geq 3$ , all applications can be achieved.

Also presented are preliminary flight test results from a Black Hawk helicopter having two flatwise-oriented accelerometers mounted on one blade. These open-loop results are to be used in the design of an active control system for rotor gust alleviation and attitude stabilization.

2. DETERMINATION OF BLADE MODAL RESPONSE

From Figures 1 and [5], the blade flatwise acceleration at station  $r$  due to response of the first two flatwise modes is

$$a(r) = (r-e)\ddot{\beta}(t) + r\dot{\alpha}^2\beta(t) + \eta(r)\ddot{\gamma}(t) + r\dot{\alpha}^2\eta'(r)g(t)$$

Then, for accelerometers mounted at  $r_1, r_2, r_3,$  and  $r_4$

$$\begin{bmatrix} a_1 \\ a_2 \\ a_3 \\ a_4 \end{bmatrix} = \begin{bmatrix} (r_1-e) & r_1\dot{\alpha}^2 & \eta(r_1) & r_1\dot{\alpha}^2\eta'(r_1) \\ (r_2-e) & r_2\dot{\alpha}^2 & \eta(r_2) & r_2\dot{\alpha}^2\eta'(r_2) \\ (r_3-e) & r_3\dot{\alpha}^2 & \eta(r_3) & r_3\dot{\alpha}^2\eta'(r_3) \\ (r_4-e) & r_4\dot{\alpha}^2 & \eta(r_4) & r_4\dot{\alpha}^2\eta'(r_4) \end{bmatrix} \begin{bmatrix} \ddot{\beta} \\ \dot{\alpha} \\ \ddot{\gamma} \\ g \end{bmatrix}$$

In matrix notation,  $A = M \cdot R$

Then the flatwise modal responses are given by

$$R = M^{-1} \cdot A$$

Note that the elements of  $M^{-1}$  are dependent only upon blade spanwise station, rotor rotation speed, and bending mode shape, i.e., they are independent of flight condition.

Similarly, the blade lag acceleration at station  $r$  due to response  $\dot{\gamma}$  of the first lag mode can be shown to be [6]

$$a_L = (r - e_L)\dot{\gamma} + e_L\dot{\alpha}^2\dot{\gamma}$$

where  $e_L$  is the spanwise location of the lag hinge. Then for accelerometers mounted at  $r_1$  and  $r_2$

$$\begin{bmatrix} a_{L1} \\ a_{L2} \end{bmatrix} = \begin{bmatrix} (r_1 - e_L) & e_L\dot{\alpha}^2 \\ (r_2 - e_L) & e_L\dot{\alpha}^2 \end{bmatrix} \cdot \begin{bmatrix} \dot{\gamma} \\ \dot{\gamma} \end{bmatrix}$$

In matrix notation  $A_L = M_L \cdot R_L$

The lag modal responses are given by

$$R_L = M_L^{-1} \cdot A_L$$

Since the elements of  $M^{-1}$  and  $M_L^{-1}$  are independent of flight condition, the solution for a desired modal response involves only the summation of the products of spanwise accelerometer signals and their corresponding constant matrix elements by an analog or digital device, here called a solver.

### 3. IDENTIFICATION OF MODAL RATE RESPONSE

Consider the block diagram shown in Figure 2. For modal acceleration  $\ddot{x}$  and modal displacement  $x$  determined as above for any mode, this diagram represents the following filter equations from [7,9]:

$$\frac{d}{dt} \hat{x} = \hat{x} + K_1(x - \hat{x}) \quad (3)$$

$$\frac{d}{dt} \hat{\dot{x}} = \ddot{x} + K_2(x - \hat{x}) \quad (4)$$

where the hatted quantities are estimated values, and  $K_1$  and  $K_2$  are constants. Writing the estimation error as

$$e = x - \hat{x}$$

and differentiating equation (3) with respect to time, there results

$$\frac{d^2}{dt^2} \hat{x} = \frac{d}{dt} \hat{x} + K_1 \dot{e} \quad (5)$$

Substituting equation (4) into equation (5),

$$\frac{d^2}{dt^2} \hat{x} = \hat{x} + K_2 e + K_1 \dot{e} \quad (6)$$

Since  $\frac{d^2}{dt^2} \hat{x} - \ddot{x} = -\ddot{e}$ , equation (6) becomes

$$\ddot{e} + K_1 \dot{e} + K_2 e = 0 \quad (7)$$

This expression represents the dynamics of the estimation error. The corresponding characteristic equation is

$$s^2 + K_1 s + K_2 = 0$$

The bandwidth and damping of the estimation process are determined by the choice of the constants  $K_1$  and  $K_2$ .

Since the elements of the filter shown in Figure 2 are independent of flight condition, the estimation of modal rate response involves only the integration of the products of constants and the measured modal responses by an analog or digital device, here called a McKillip filter. Note that an improved estimate of the modal displacement  $x$  is also obtained due to the double integration of modal acceleration  $\ddot{x}$  embodied in the filter. Also, note that no knowledge of the rotor or its flight condition is required in designing the filter.

### 4. FORM OF THE MODAL CONTROLLER

As discussed in the Introduction, the modal controller voltage output to the blade pitch actuator is proportional to modal acceleration, rate, and displacement:

$$V = -K_A \ddot{x} - K_R \dot{x} - K_P x$$

where  $K_A$ ,  $K_R$ , and  $K_P$  are constants and therefore independent of flight condition.

For modal damping augmentation only,

$$V = -K_R \dot{x}$$

### 5. MODAL CONTROL BY INDIVIDUAL- BLADE- CONTROL (IBC)

The solver, McKillip filter, and controller described in Sections 2-4 are combined to form the IBC system for a given mode. The combined functions of the solver and the McKillip filter are here called the "observer". Some applications are described below, including experimental results obtained at MIT from a four-foot-diameter wind tunnel model rotor, using IBC.

Reference [3] describes the application of IBC to helicopter gust alleviation. The feedback blade pitch control was proportional to blade flapping acceleration and displacement, i.e.,

$$\Delta\theta = -K \left( \frac{\beta}{\Omega^2} + \beta \right)$$

A block diagram of the control system is shown in Figure 3. Note that each blade requires only two flatwise-oriented blade-mounted accelerometers.

Figure 4 shows the effect of increasing the open-loop gain  $K$  upon the IBC gust alleviation system performance. Note that the experimental reduction in gust-induced flapping response is in accordance with the theoretical closed-loop gain  $1/(1+K)$ .

The Lock number of the model blade was 3.0. For a full size rotor, the increase in damping due to the increase in Lock number results in the flapping at excitation frequency becoming the dominant response. Also, with increased blade damping it becomes possible to use higher feedback gain for the same stability level, and as a consequence the IBC system performance improves with increasing Lock number.

Following the successful alleviation of gust disturbances using the IBC system, Reference [3] showed the theoretical equivalence of blade flapping response due to atmospheric turbulence and that due to other low-frequency disturbances, e.g., helicopter pitch and roll attitude; therefore these disturbances can also be alleviated by the IBC system, as shown in [8], to provide helicopter attitude stabilization.

References [5,8] describe the application of IBC to rotor vibration alleviation. The feedback blade pitch control was proportional to blade bending acceleration, rate and displacement, i.e.,

$$\Delta\theta = -K_A \ddot{\psi} - K_R \dot{\psi} - K_P \psi$$

A block diagram of the system is shown in Figure 5. Note that each blade requires four flatwise-oriented blade-mounted accelerometers.

Preliminary experimental results presented in Figure 6 show the effect of increasing the IBC open-loop gain  $K$  from 0 to 3 upon the flatwise bending mode response. Note that the experimental reduction in vibratory bending response is in accordance with the theoretical closed-loop gain  $1/(1+K)$ .

Since a major source of helicopter higher harmonic vertical vibration is the blade flatwise bending response to the impulsive loading due to blade-vortex or blade-fuselage interaction, if the blade flatwise bending response is controlled, the higher harmonic vertical vibration will be correspondingly reduced, as shown in Figure 7, from [11].

It should be noted that suppression of blade flapping and flatwise bending responses and their corresponding in-plane Coriolis forces will tend to alleviate in-plane vibration as a beneficial by-product of vertical vibration alleviation.

Reference [6] describes the application of IBC to rotor lag damping augmentation. The feedback voltage to the blade pitch control actuator was proportional to blade lag rate, i.e.,

$$\tau V + V = -K_R \dot{\psi}$$

where the time delay is required for closed-loop stability. A block diagram of the system is shown in Figure 8. Note that each blade requires two lagwise-oriented blade-mounted accelerometers.

Figure 9 shows the effect of increasing the IBC open-loop gain on experimental blade lag damping. The figure shows a rotation of the slope of the phase angle versus frequency curve at lag resonance, in the direction of increased lag damping, as  $K_R$  is increased. The increase in lag damping ratio due to the control system was determined to be 0.37.

The preceding sections have demonstrated that the use of blade-mounted accelerometers as sensors makes possible the control of the flapping, flatwise bending, and lag modes of each blade individually. This control technique is applicable to helicopter rotor gust alleviation, attitude stabilization, vibration alleviation, and lag damping augmentation.

For rotors having three blades, any arbitrary pitch time history can be applied to each blade individually using the conventional swash plate. Rotors with more than three blades require individual actuators for each blade for some applications; other applications such as gust alleviation, attitude stabilization, vibration alleviation, and 1P lag damping augmentation can be achieved using a conventional swash plate, as shown below and in [8].

If the control requirement for the  $m$ th blade of an  $N$ -bladed rotor is  $\theta_m$ , determined using blade-mounted accelerometers as described in Section 2, then the corresponding control requirement for the swash plate is

$$\theta = \theta_0 + \theta_{1c} \cos \psi + \theta_{1s} \sin \psi + \theta_2$$

Using the mathematics of [12], P. 351, the control laws are

$$\theta_0 = \frac{1}{N} \sum_{m=1}^N \theta_m = 0 \text{ unless } n = pN$$

$$\theta_{1c} = \frac{2}{N} \sum_{m=1}^N \theta_m \cos \psi_m = 0 \text{ unless } n = pN \pm 1$$

$$\theta_{1s} = \frac{2}{N} \sum_{m=1}^N \theta_m \sin \psi_m = 0 \text{ unless } n = pN \pm 1$$

$$\theta_2 = 0 \text{ unless } n = pN \pm N/2 \text{ [12], P. 348}$$

where  $p$  = any integer  
 $n$  = rotor harmonic number

The physical significance of the above equations is that IBC of an  $N$ -bladed rotor having a conventional swash plate is possible for those IBC functions involving the zeroth (quasi-steady), first,  $N$ th, and  $(N \pm 1)$ th harmonics of rotor speed, e.g., gust alleviation ( $p=0$ ), attitude stabilization ( $p=0$ ), vibration alleviation ( $p=1$ ), and 1P lag damping augmentation ( $p=0$ ).

Note that all harmonics and in general any arbitrary time history of control are achievable with a three-bladed rotor using a conventional swash plate.

The summations of individual blade sensor signals required to obtain the swash plate collective and cyclic pitch components provide a filtering action such that only the desired harmonics  $0P$ ,  $1P$ ,  $NP$ , and  $(N \pm 1)P$  remain after summation, i.e., no specific harmonic analysis is required.

Since all sensing is done in the blades, no transfer matrices from non-rotating to rotating system are required; therefore no updating of these matrices is required, and no non-linearity problems result from the linearization required to obtain the transfer matrices. Also, blade state measurements allow tighter vehicle control since rotor control can lead fuselage response: this lead should provide more effective gust alleviation and permit higher control authority without inducing rotor instabilities than would be possible without rotor state feedback [13].

A block diagram of an active control system for the conventional swash plate of a helicopter rotor having four blades A, B, C, and D is shown in Figure 10. The control voltages  $V_{A-D}$  are generated from blade-mounted accelerometer signals, as described in preceding sections. A schematic showing all the components of such an active control system is shown in Figure 11 for the special case of vibration alleviation.

Recently, the first phase of a joint NASA-U.S. Army flight test program involving the UH-60A Black Hawk helicopter was completed. The flight test program, conducted from January through June 1987 at Edwards Air Force Base, California, was part of the NASA Ames Research Center's Modern Technology Rotors Program (MTR). The MTR program calls for a series of flight investigations using current, state-of-the-art rotor systems. The present program, involving the UH-60A Black Hawk, is the first of two phases to be carried out by NASA, in conjunction with the U.S. Army Aviation Engineering Flight Activity (USAAEFA). The Phase I flight program included an evaluation of rotor aerodynamic limits, handling qualities and baseline acoustic measurements of the UH-60A. It should be noted that the flight data contained herein are preliminary in nature.

The instrumentation for this flight test included a variety of aircraft state and operating condition sensors, hub and fuselage accelerometers, and a strain-gauge-equipped blade. The strain-gauged blade also carried a blade motion sensor system capable of independently measuring blade position, and two blade-mounted accelerometers. The accelerometers used during the flight test program were Entran Model EGA-125-D (damped), and were located near the root and the tip of the blade, as shown in Figure 12. The root and tip accelerometers had ranges of  $\pm 3g$  and  $\pm 250g$ , respectively. The accelerometers were mounted along the blade feathering axis to reduce pitch coupling effects. The mounting angles of the accelerometers relative to the blade were chosen to best reflect a variety of flight speeds and conditions, i.e., blade collective settings. Therefore, the accelerometers were placed such that at mid-collective position, they were at zero pitch angle and their sensitive axes were in the blade-flapping direction. This arrangement is depicted in Figure 13.

The sensor used to independently determine blade position was the Sikorsky blade-relative-motion hardware system. This unit allows measurement of blade-flapping angle at the blade root, relative to the main rotor shaft axis. The blade-motion system also allows measurement of the blade root pitch and lead-lag angles.

The data acquisition system used during the UH-60A flight test program was the USAAEFA HiCap PCM data system. Both accelerometers and the independent main rotor flapping sensor were sampled at a rate of 517 samples per second. This rate allowed reliable resolution of the data up to 80 Hz. Since the rotor rotational speed of the UH-60A is roughly 4.3 Hz, the data sampling rate provided information well beyond the present frequency range of interest (5P and below).

## 8. FLIGHT TEST RESULTS AND DISCUSSION

The objective of the flight measurements was to compare the root and tip acceleration measurements with values predicted by the simple rigid-blade model and to compare estimated flapping with that measured by the root-mounted flapping transducer.

Figures 14 and 15 show the time histories and frequency spectra of the two accelerometers and the flapping transducer for an 80 kt. level flight trim condition of the UH-60A helicopter. Multiple harmonics of rotor speed (4.3 Hz) are evident in the record, with 1P and 3P contributions being particularly strong. In order to estimate flapping for purposes of controlling flight dynamics, only the lower frequency responses at 0-1P are of interest. The accelerometer spectra, however, indicate significant 1P response due to bending, implying the likelihood of additional contributions to the local values of blade slope and blade acceleration, which together determine the accelerometer responses.

For simple harmonic motion of a rigid blade at 1P with mean flapping  $\beta_0$  and  $\beta_1$  <sup>amplitude</sup>, the expected accelerometer response is easily calculated. Using the measured flapping values for an 80 kt. trim, the estimated and measured

tip acceleration are shown in Fig. 16(a). The result indicates that the amplitude of the measured tip acceleration response is greater than the simple model prediction by a factor of five. It is likely that the increased output is due to the local slope and acceleration due to blade bending. The root accelerometer output was almost identical to the expected response, as shown in Figure 16(b).

The measurements showed a significant phase shift between tip and root accelerometer signals [Fig. 16(c)]. The tip signal appears to lead the root signal by 50 to 60 degrees of rotor azimuth in some flight conditions, and this lead was present in all the data to some degree. Independent confirmation of the existence of phase differences due to bending can be seen in the analysis of CH-34 blade response calculations by Esculier and Bouzman [14].

The following analysis, including blade bending in the accelerometer signal, shows the physical basis for the above phenomena.

The flatwise accelerometer signal including blade bending is

$$\frac{a_F}{R\Omega^2} = (x-\xi) \frac{\ddot{\beta}}{\Omega^2} + x\beta + \frac{\eta(x)}{R} \frac{\ddot{g}(t)}{\Omega^2} + x \frac{\eta'(x)}{R} g(t) \quad (8)$$

where  $\eta(x)$  = bending mode shape  
 $g(t)$  = bending mode displacement

Assume  $\beta = \bar{\beta} e^{i\omega t}$ ;  $g = \bar{g} e^{i\omega t}$ ;  $\frac{a_F}{R\Omega^2} = \frac{\bar{a}_F}{R\Omega^2} e^{i\omega t}$  where  $\bar{\beta}$  and  $\bar{g}$  are

complex to account for phase. Also take

$$\eta(x) = 4 \left( \frac{x-\xi}{1-\xi} \right)^2 - 3 \left( \frac{x-\xi}{1-\xi} \right)$$

$$\therefore \eta'(x) = \frac{1}{1-\xi} \left[ 8 \left( \frac{x-\xi}{1-\xi} \right) - 3 \right]$$

$$\therefore \frac{\bar{a}_F}{R\Omega^2} = - (x-\xi) \left( \frac{\omega}{\Omega} \right)^2 \bar{\beta} + x\bar{\beta} - \eta(x) \left( \frac{\omega}{\Omega} \right)^2 \bar{g} + x\eta'(x)\bar{g} \quad (9)$$

For  $\frac{\omega}{\Omega} = 1$ , equation (9) becomes

$$\frac{\bar{a}_F}{R\Omega^2} = \xi \bar{\beta}_1 + f(x,\xi) \bar{g}_1 \quad (10)$$

where  $f(x,\xi) = \left[ 4 \left( \frac{x}{1-\xi} \right)^2 - 4 \left( \frac{\xi}{1-\xi} \right)^2 - 3 \left( \frac{\xi}{1-\xi} \right) \right]$

Equation (10) indicates that the blade-bending contribution to the accelerometer 1P signal increases as the square of the spanwise accelerometer location  $x$ , while the flapping 1P contribution is invariant with span. For the data of Figure 15, the following 1P flapping and bending amplitudes were estimated, using equation (10):

$$\left| \bar{\beta}_1 \right| = 0.044 \text{ rad.}$$

$$\left| \bar{g}_1 \right| = 0.0038$$

Then  $\xi \left| \bar{\beta}_1 \right| = 0.0021$

$$f(x,\xi) \left| \bar{g}_1 \right| = -0.00050 \text{ (inboard)}$$

$$f(x,\xi) \left| \bar{g}_1 \right| = 0.015 \text{ (outboard)}$$

It is seen from equation (2) that the inboard 1P accelerometer signal is flapping-dominated, while the outboard 1P accelerometer signal is bending-dominated.

For 1P excitation, blade bending (natural frequency  $\approx 3P$ ) has a small phase lag, and flapping (natural frequency  $\approx 1P$ ) has a large phase lag. Therefore the bending-dominated tip accelerometer signal 1P component can

be expected to have a substantial lead over that of the flapping-dominated root accelerometer signal.

The above results suggest that blade 0-1P flapping estimation can be accomplished by using two inboard accelerometers to minimize the blade bending contribution to the accelerometer signals. Alternatively, the blade flapping and bending response can be determined by using four spanwise accelerometers and the methodology of Section 2 to solve for flapping and/or bending response.

## 9. CONCLUSIONS

1. The flight test results described above indicate that the use of blade-mounted accelerometers to estimate blade flapping and flatwise bending is feasible in terms of signal size and repeatability.
2. Inboard 0-1P accelerometer signals are flapping-dominated.
3. Outboard 0-1P accelerometer signals are bending-dominated.
4. Blade 0-1P flapping estimation can be accomplished by using two inboard accelerometers to minimize the bending contribution to the accelerometer signals.
5. Blade 0-1P flapping and bending estimation can be accomplished by using four accelerometers. In this case, the bending contribution to the accelerometer signals can be accounted for in estimating blade flapping.

## REFERENCES

1. Kretz, M., "Research in Multicyclic and Active Control of Rotary Wings," *Vertica* 1, 95-105, 1976.
2. Ham, N.D., "A Simple System for Helicopter Individual-Blade-Control Using Modal Decomposition", *Vertica*, 4, 23-28, 1980.
3. Ham, N.D. and McKillip, R.M., Jr., "A Simple System for Helicopter Individual-Blade-Control and Its Application to Gust Alleviation", *Proc. Thirty-Sixth AHS Annual National Forum*, Washington, D.C., May 1980.
4. Ham, N.D. and Quackenbush, T.R., "A Simple System for Helicopter Individual-Blade-Control and Its Application to Stall-Induced Vibration Alleviation", *Proc. AHS National Specialists' Meeting on Helicopter Vibration*, Hartford, CT, November 1981.
5. Ham, N.D., "Helicopter Individual-Blade-Control and Its Applications", *Proc. Thirty-Ninth AHS Annual National Forum*, St. Louis, MO, May 1983.
6. Ham, N.D., Behal, Brigitte L. and McKillip, R.M., Jr., "Helicopter Rotor Lag Damping Augmentation Through Individual-Blade-Control", *Vertica*, 7, 361-371, 1983.
7. McKillip, R.M. Jr., "Periodic Control of the Individual-Blade-Control Helicopter Rotor", *Vertica*, 9, 199-224, 1985.
8. Ham, N.D., "Helicopter Gust Alleviation, Attitude Stabilization, and Vibration Alleviation Using Individual-Blade-Control Through a Conventional Swash Plate", *Proc. Forty-First AHS Annual National Forum*, Fort Worth, Texas, May 1985.
9. McKillip, R.M. Jr., "Kinematic Observers for Rotor Vibration Control", *Proc. Forty-Second AHS Annual National Forum*, June 1986.
10. Ham, N.D., "Helicopter Individual-Blade-Control Research at MIT 1977-1985," *Vertica* 11, 109-122, 1987.
11. Leone, P.F., "A Method for Reducing Helicopter Vibration," *JABS* 2, 3, July 1957.
12. Johnson, W., *Helicopter Theory*, Princeton U.P., 1980.
13. DuVal, R.W., "Use of Multiblade Sensors for On-Line Rotor Tip-Path-Plane Estimation," *JABS* 25, 4, October 1980.
14. Esculier, J.E., and Bouzman, W.G., "Calculated and Measured Blade Structural Response on a Full-Scale Rotor", *Proc. Forty-Second AHS Annual National Forum*, Washington, D.C. 1986.

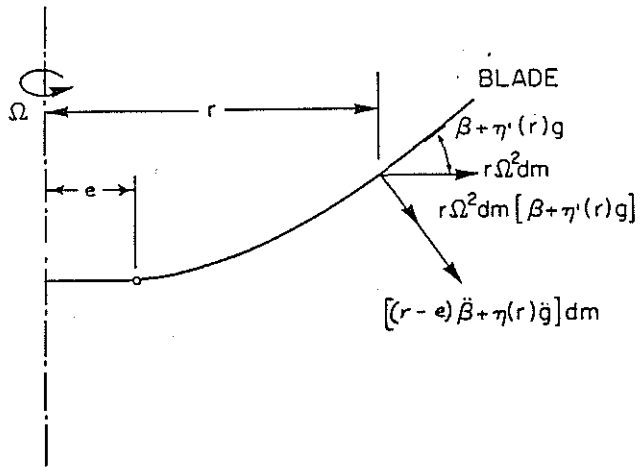


Figure 1. Blade Flatwise Inertia Forces

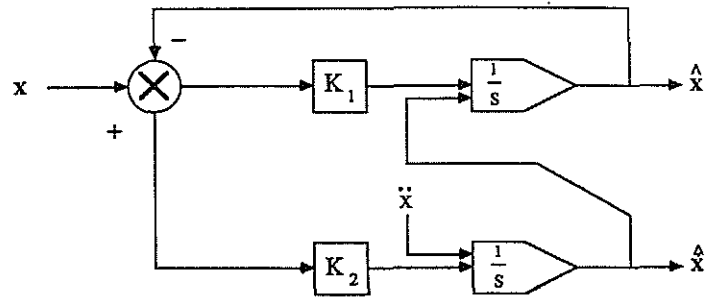


Figure 2. Block Diagram of McKillip Filter

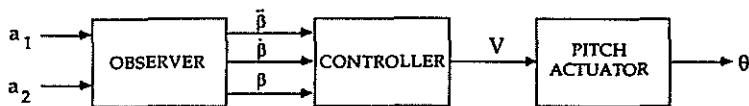


Figure 3. Block Diagram of Flapping IBC System

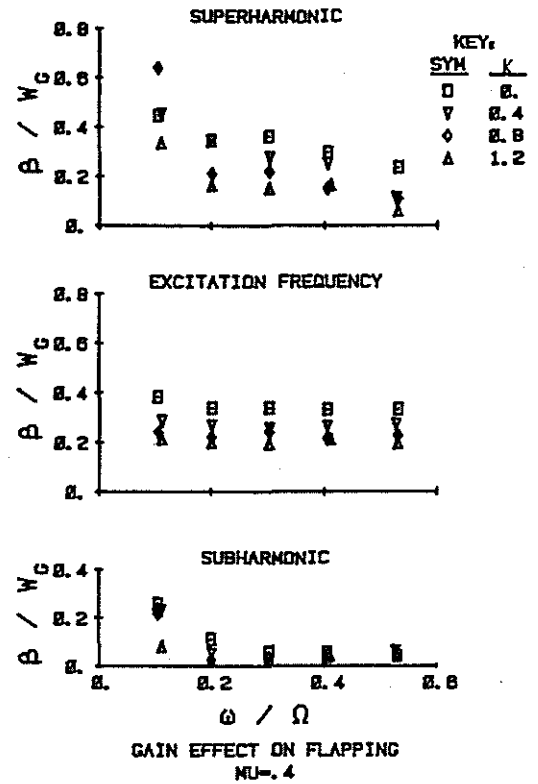


Figure 4. Effect of Feedback Gain on Flapping Response to Gust ( $\nu = 0.4$ )



Figure 5. Block Diagram of Bending IBC System

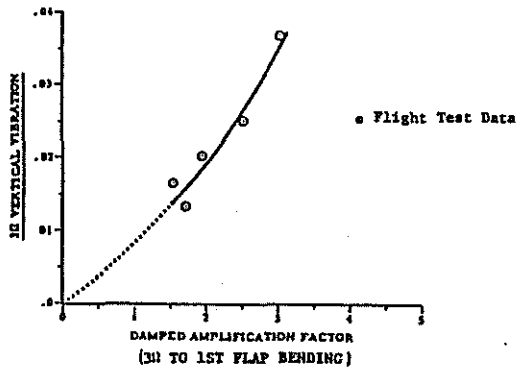


Figure 7. Effect of Blade Bending Amplification Factor on Maximum Cockpit Vibration Level

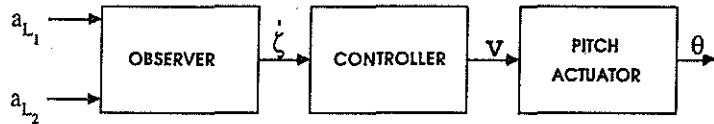


Figure 8. Block Diagram of Lag IBC System

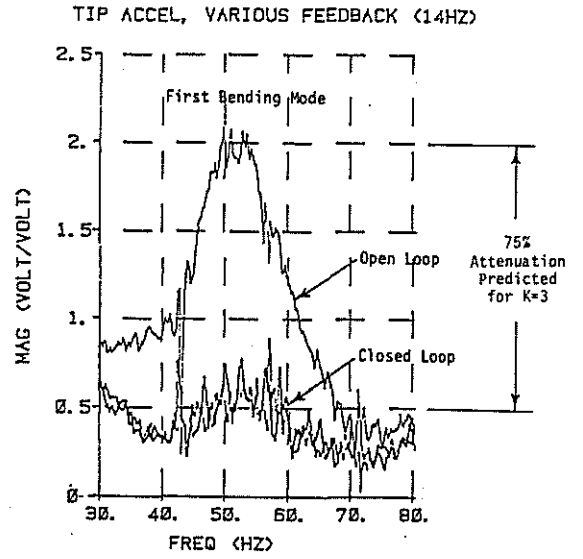


Figure 6. Open and Closed Loop Flatwise Tip Accelerometer Response to White Noise Pitch Input in Hover

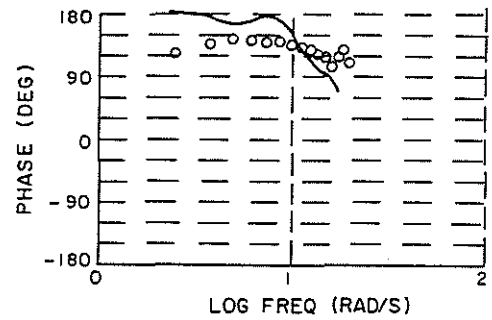
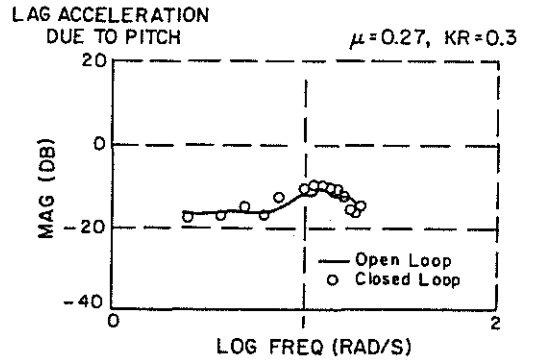


Figure 9. Open and Closed Loop Acceleration Response to White Noise Pitch Input ( $\mu = 0.27$ )

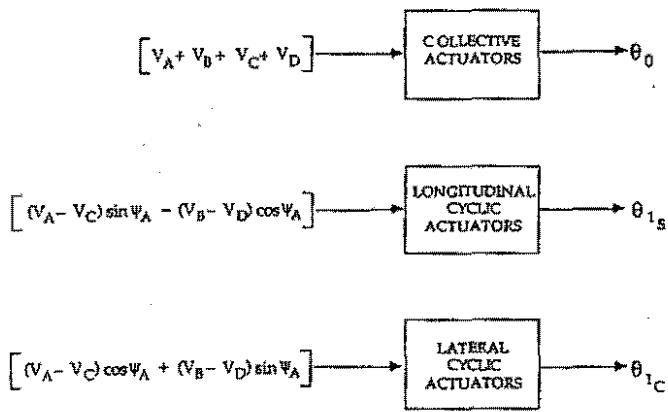


Figure 10. Block Diagram of Flapping, Bending, or Lag Control System Using the Conventional Swash Plate: Four-Bladed Rotor

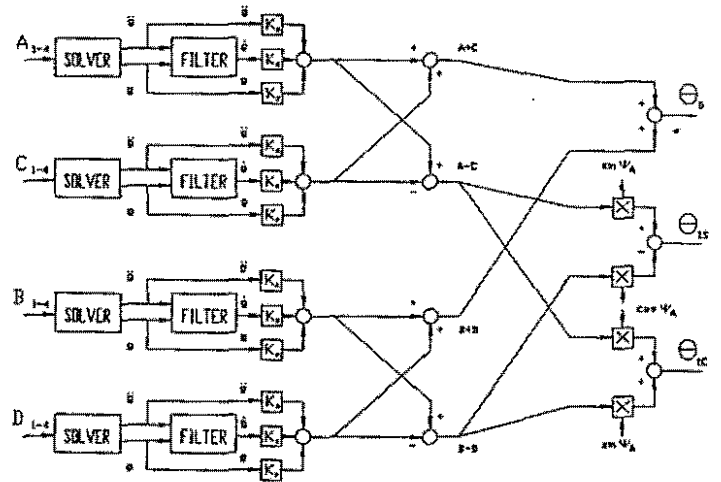


Figure 11. Schematic of Bending Control System Using the Conventional Swash Plate: Four-Bladed Rotor (Drawn by R.M. McKillip Jr.)

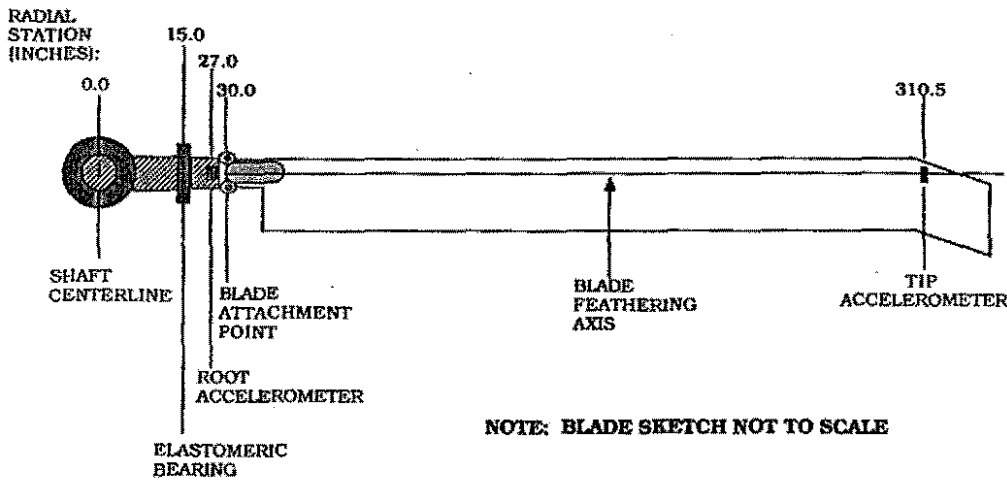


Figure 12. Root and Tip Accelerometer Locations on UH-60A Blade

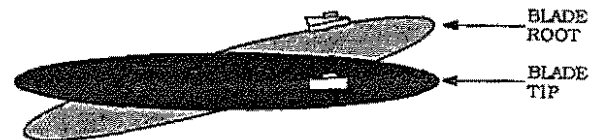


Figure 13. Relative Mounting Positions of Root and Tip Accelerometer

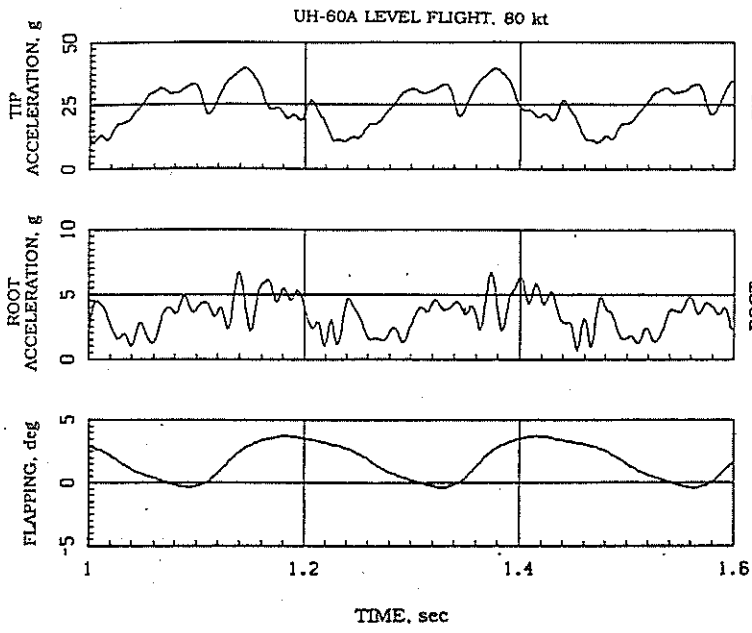


Figure 14. Typical Flapping Transducer and Accelerometer Time Histories

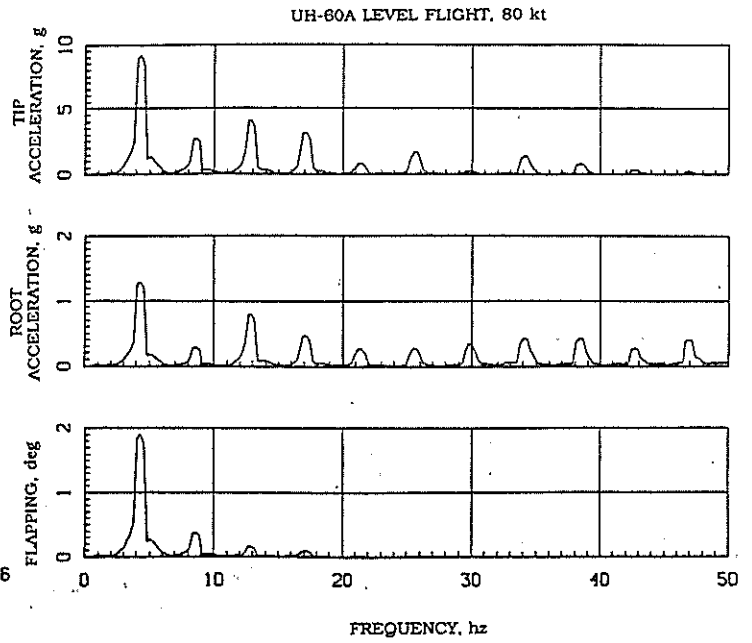


Figure 15. Typical Flapping Transducer and Accelerometer Frequency Spectra

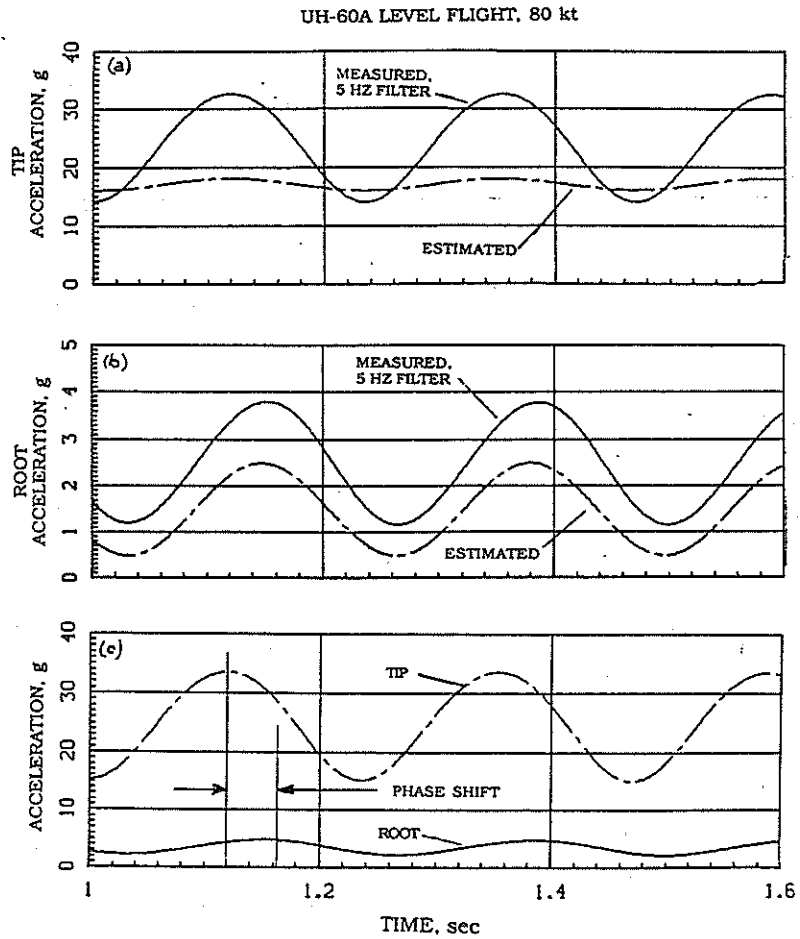


Figure 16. Estimated Rigid-Blade-Model and Measured 1P Accelerometer Time Histories